DE86004169

CO + H SUB 2 REACTION OVER NITROGEN-MODIFIED IRON CATALYSTS. QUARTERLY TECHNICAL PROGRESS REPORT, APRIL 1-SEPTEMBER 30, 1985

PURDUE UNIV., LAFAYETTE, IN. SCHOOL OF
CHEMICAL ENGINEERING

DEC 1985

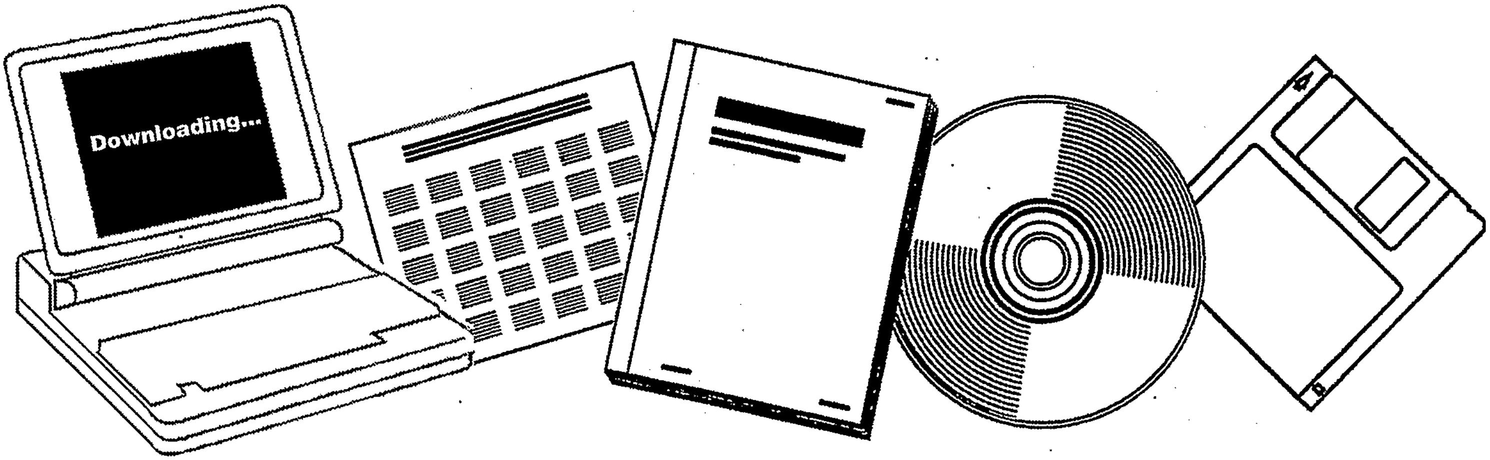

One Source. One Search. One Solution.

NTIS

Providing Permanent, Easy Access to U.S. Government Information

National Technical Information Service is the nation's largest repository and disseminator of government-initiated scientific, technical, engineering, and related business information. The NTIS collection includes almost 3,000,000 information products in a variety of formats: electronic download, online access, CD-ROM, magnetic tape, diskette, multimedia, microfiche and paper.

Search the NTIS Database from 1990 forward

NTIS has upgraded its bibliographic database system and has made all entries since 1990 searchable on **www.ntis.gov.** You now have access to information on more than 600,000 government research information products from this web site.

Link to Full Text Documents at Government Web Sites

Because many Government agencies have their most recent reports available on their own web site, we have added links directly to these reports. When available, you will see a link on the right side of the bibliographic screen.

Download Publications (1997 - Present)

NTIS can now provides the full text of reports as downloadable PDF files. This means that when an agency stops maintaining a report on the web, NTIS will offer a downloadable version. There is a nominal fee for each download for most publications.

For more information visit our website:

www.ntis.gov

U.S. DEPARTMENT OF COMMERCE
Technology Administration
National Technical Information Service
Springfield, VA 22161

DOE/PC/50804--11

DE86 004169

DOE/PC/50804-11,12

$CO + H_2$ Reaction Over Nitrogen-Modified Iron Catalysts

Quarterly Technical Progress Report
for the Period Apr. 1, 1985 - Sept. 31, 1985

W. Nicholas Delgass
Purdue University
West Lafayette, Indiana 47907

PREPARED FOR THE

U.S. DEPARTMENT OF ENERGY

DISCLAIMER

Disclaimer

TABLE OF CONTENTS

LIST OF FIGURES AND TABLES

ABSTRACT

A 4.5 wt% iron supported on Carbolac - 1 catalyst was prepared by incipient wetness and characterized by in-situ Mössbauer spectroscopy. The reduced catalyst exhibited superparamagnetic iron at RT as well as extreme sensitivity to oxygen. Both of these results are indicative of small (~20Å), very highly dispersed iron crystallites. After nitriding to ξ–Fe_2N followed by Fischer-Tropsch synthesis (with 3:1 H_2 /CO at 250 °C) for 20 hrs, the sample was re-reduced in H_2 for 8 hrs at 400 °C. The re-reduced spectrum showed that ~84% of the iron appeared to be bulk-like, indicating that the reaction environment can induce iron migration on the catalyst.

Computer simulation of the decomposition of a γ–Fe_4N catalyst in hydrogen at 523 K indicates that the observed ammonia evolution curve can be modeled by a two step process. The model incorporates a conversion from a homogeneous mixture of nitrogen in the core into a surface nitrogen species, which is subsequently hydrogenated to ammonia. The model demonstrates that competition between this nitrogen surface species and adsorbed hydrogen for the available surface sites can account for the maximum in the observed NH_3 evolution rate. Other models incorporating shrinking core distributions of nitrogen in the core failed to fit the experimental results.

1. *OBJECTIVES AND SCOPE*

1.1 BACKGROUND

The feasibility of utilizing synthesis gas ($CO+H_2$) via the Fischer-Tropsch reaction pathway for the production of fuels and chemicals is well established. The SASOL ventures, for example, take advantage of abundant coal resources to produce both desirable synthetic automotive fuels and basic chemical feedstocks. The applicability of these chemical transformations is nonetheless limited. The present procedure requires extensive processing if the production of non-essential byproducts is to be avoided. The discovery and subsequent usage of improved catalysts would therefore be advantageous.

Experimental results published in the current literature show that nitrogen affects the performance of iron catalysts-catalysts which find widespread use in the Fischer-Tropsch synthesis route. Prenitriding of the iron catalyst has been reported to shift the product distribution to one exhibiting lower molecular weight fractions and enhanced alcohol yields (1). On the other hand, simultaneous introduction of ammonia (NH_3) with synthesis gas produces nitrogeneous compounds (2, 3, 4). Furthermore, and probably of greater importance, this addition of ammonia effects a reduction in the overall chain length of compounds in the product spectrum (2). It is of considerable interest, therefore, to study these and other characteristics of nitrided iron catalysts in order to gain a basic understanding of their behavior. Discovery of the new pathways in Fischer-Tropsch synthesis afforded by nitrogen will add to the fundamental knowledge from which future synthesis catalysts can be derived.

1.2 OBJECTIVES

The scope of the program may be broken down into two main areas of concern. Firstly, consideration must be given to the role of the surface nitrogen in

i. altering the product distribution and

ii. stabilizing catalyst activity

of the synthesis reactions. *In-situ* Mössbauer studies identify the various iron nitride phases and allow for examination of their stability during reaction. The Mössbauer results form the basis for detailed kinetic tracer experiments involving transient and isotope labeling analyses. Ultrahigh vacuum work using SIMS and AES will supplement the Mössbauer and kinetic characterizations.

The second area of consideration involves the kinetic and catalytic effects observed during the addition of ammonia to the synthesis gas stream. Transient work is ideal for observing initial activity changes occurring as a result of NH_3 pulses. Along with ultrahigh vacuum studies, the transient kinetics of NH_3 addition will help clarify which steady state experiments would be most productive. The various analytical methods will define interactions between surface and bulk nitrogen, and their role in effecting new reaction pathways.

The primary experiments which define our route to understanding which parameters influence the selectivity and alter the activity of synthesis reactions may, therefore, be outlined as follows:

i. Mössbauer and simultaneous kinetics of prenitrided iron catalysts will be used to determine nitride phase stability and to correlate these phases to reaction selectivity. The initial pressure of one atmosphere may later be increased.

ii. Similar analysis of the effects of addition of NH_3 to the reactant stream will be performed.

iii. Transient analysis and isotope tracer studies of synthesis reactions over prenitrided catalysts will determine surface nitride stability. The stoichiometry at the surface and influence of nitriding on CO dissociation will be sought.

iv. Ultrahigh vacuum analysis will examine surface stoichiometry and reaction intermediates. Interaction between the nitrided phases and adsorption bond strengths of CO and H_2 will be investigated.

v. The effects of NH_3 addition to the reactant stream will be similarly followed by UHV and transient tracer studies to determine possible alterations in reaction pathways invoked by the presence of NH_3.

Computer modeling will be undertaken to aid in quantitative interpretation of transient data.

2. TECHNICAL PROGRESS

2.1 Summary of results

In this report, we consider computer simulation of different proposed models for the decomposition of a γ'-Fe_4N catalyst in hydrogen into α-Fe and NH_3 at 523K. The experimental results, which we presented in an earlier report (5), indicated a slow activation of the decomposition reaction: Ammonia produced from the catalyst built slowly to a maximum only after approximately 100 seconds. Intuitively, we can rule out nitrogen diffusion within the catalyst bulk as the sole rate limiting step, since this process would have the highest rate at the start of the reaction. Likewise, a single rate limiting surface reaction would build to a steady state decomposition rate which is also not observed.

Relatively simple models combining a number of reaction steps can be written for the catalyst system in a CSTR. We have found that the experimentally observed ammonia decomposition rate can be qualitatively reproduced by a model incorporating a step to convert bulk nitride to surface nitrogen followed by subsequent hydrogenation of the surface nitrogen species. In the model, surface nitrogen dominates the surface at the start of the reaction, effectively blocking out surface hydrogen, and thus the rate of ammonia production is low. As the bulk nitride concentration decreases, so does the surface nitrogen, thus allowing for more surface hydrogen and higher surface reaction rates to ammonia. Finally, the conversion from nitride to surface nitrogen limits the reaction as the nitride concentration becomes small. Other models incorporating diffusion or shrinking core approximations could not fit the experimental results.

Also in this reporting period, a 4.5 wt% iron supported on Carbolac - 1 catalyst was prepared by incipient wetness and characterized by in-situ Mössbauer spectroscopy. The reduced catalyst exhibited superparamagnetic iron at RT as well as extreme sensitivity to oxygen. Both of these results are indicative of small (~20Å), very highly dispersed iron crystallites. After nitriding to ξ–Fe_2N followed by Fischer-Tropsch synthesis (with 3:1 H_2/CO at 250 °C) for 20 hrs, the sample was re-reduced in H_2 for 8 hrs at 400 °C. The re-reduced spectrum showed that ~84% of the iron appeared to be bulk-like, indicating that the reaction environment can induce iron migration on the catalyst.

2.2 Computer Simulation of Denitriding in Hydrogen

In a previous report (5), we presented the experimental result for the decomposition of γ'–Fe_4N in hydrogen at 523K. The ammonia curve, reproduced as the "experimental" line in Figure 1, indicates two distinct maxima. The first small spike is primarily from an active surface species and the second large maximum is from hydrogenation of nitrogen from the bulk. The bulk hydrogenation exhibits an "autocatalytic" phenomenon in which the rate steadily increases over a long period. This behavior immediately rules out simple models for the reaction mechanism. If the reaction were limited by the diffusion of nitrogen to the surface from the bulk, the reaction would proceed at the maximum rate and decrease thereafter. Likewise, a surface reaction

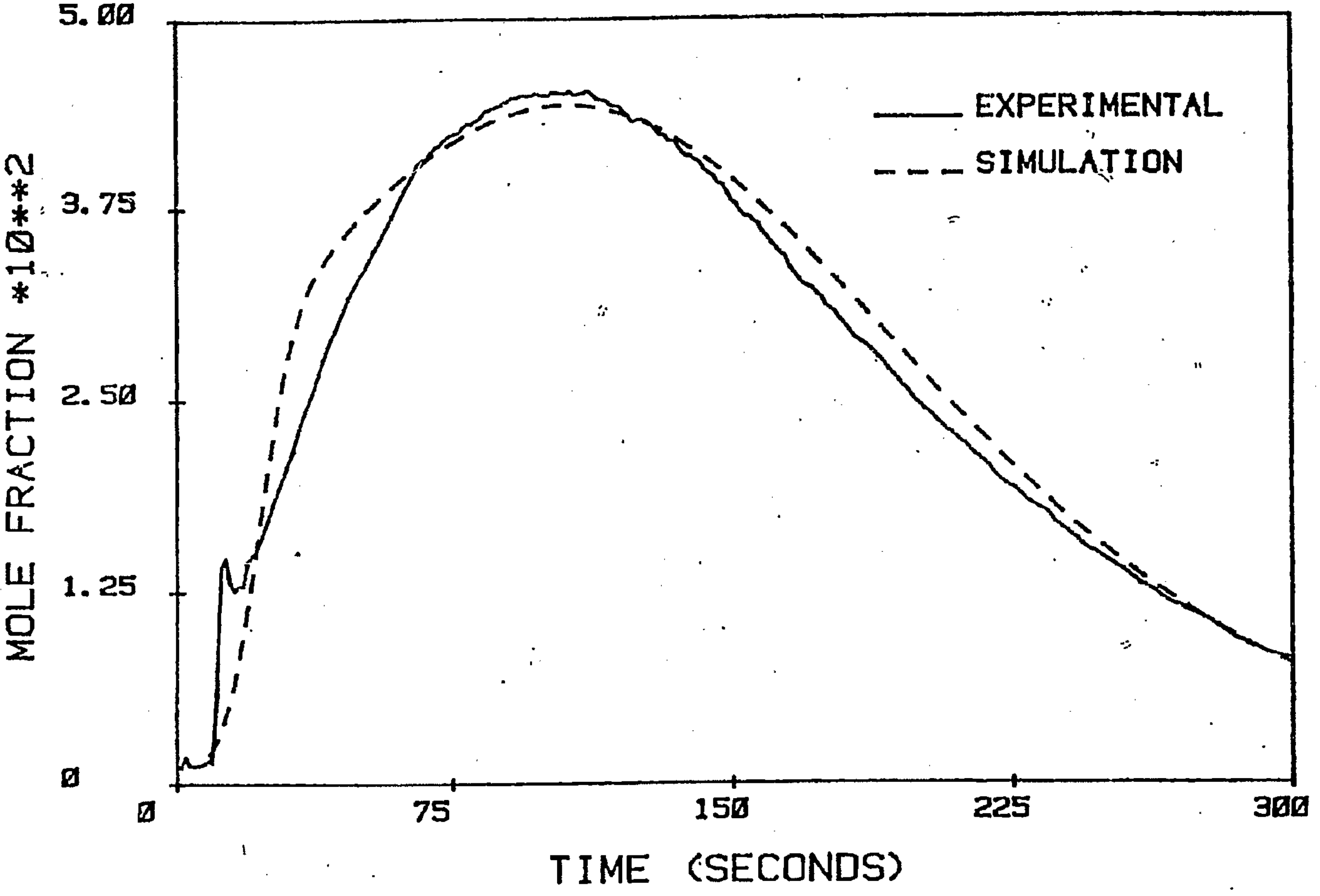

Figure 1 Simulation of the Decomposition of γ'-Fe_4N in Hydrogen: Homogeneous Core Model

limiting would quickly come to steady state and evolve ammonia at a constant rate.

Since neither a simple bulk diffusion model nor an equilibrium surface reaction model will predict the behavior observed in Figure 1, a model incorporating both the bulk conversion to surface nitrogen and the subsequent reaction must be proposed to explain the "autocatalytic" phenomenon. For the first approximation, the surface area and the reaction rate constants are assumed to be constant during the entire decomposition. Since the surface of γ'–Fe_4N is the first to be converted to α-Fe, this is not an unreasonable assumption. For the higher nitrides (ϵ and ς), however, the surface may not convert to the α phase immediately, since the decomposition rate is significantly different for these catalysts.

The simplest model for this process involves only two key reaction steps and an equilibrium step:

$$N_{nitride} + s \xrightarrow{k_1} N_{surf} \tag{1}$$

$$N_{surf} + H_{surf} \xrightarrow{k_2} NH_{surf} \tag{2}$$

$$NH_{surf} + 2H_{surf} \xrightarrow{fast} NH_3 \tag{3}$$

$$H_2 + 2s \overset{K}{\rightleftarrows} 2H_{surf} \qquad (4)$$

The fast step does not affect the production rate of NH_3.

For the calculation of hydrogen surface coverage, the adsorption/desorption processes are assumed to be in equilibrium. These processes are very fast compared to surface reaction rates to produce ammonia. The rate, with appropriate activation energy and preexponential factor, for hydrogen desorption from iron at temperatures around 400 K is given by Benziger, et al. (6) as:

$$\text{rate} = (1.5 \text{ x } 10^{-2} \text{ cm}^2/\text{atom s})\sigma_H^2 \cdot \exp(-86.6(\text{Kcal/mol})/RT) \qquad (5)$$

where σ_H is the coverage of hydrogen in atoms/cm^2. The adsorption is assumed to proceed through an unactivated process at the collision frequency with an empty site, given by:

$$\text{rate} = 1/4 \text{ v } n_{H_2} n_s \qquad (6)$$

where v is the velocity and n_{H_2} is the density of H_2 at reaction conditions, 523 K. By undimensionalizing the factors N, n_s and σ_H, the equilibrium constant K is obtained by equating these two rates at 523 K such that:

$$K = \frac{(H_{surf})^2}{(S)^2(H_2)} = \frac{k_{ads}}{k_{des}} = 1584 \qquad (7)$$

The sites available for hydrogen adsorption are those not occupied by nitrogen, since NH_x species are very reactive and present only in small quantities. By a total site balance:

$$(H_{surf}) + (S) + (N_{surf}) = 1 \qquad (8)$$

Since N_{surf} is known at any time step in the simulation, we can combine equations (7) and (8) to solve for (S) and (H_{surf}) in terms of N_{surf} :

$$S = 0.03(1-N_{surf}) \tag{9}$$

$$H_{surf} = 0.97(1-N_{surf}) \tag{10}$$

These last two equations describe the hydrogen surface coverage during the simulation.

In the simulation, the nitrogen surface coverage is determined by the numerical solution to the differential equations describing the model. The corresponding hydrogen surface coverage and empty sites are determined as a function of the surface not occupied by nitrogen. Physically this corresponds to rapid surface hydrogen adjustment to changes due to the two reaction steps (1) and (2) during an individual time step. In essence, the time it takes to adsorb and desorb hydrogen is assumed to be infinitely faster than the rates of change of nitrogen reactive intermediates.

For the first approximation, the initial spike of ammonia is not considered, since this fast reaction might indeed be of the same speed as hydrogen adsorption, and thus the assumption of equilibrium for hydrogen would be invalid. Furthermore, the addition of the reaction steps for this species would necessitate the mathematical modeling of an extremely stiff set of differential equations, which is possible but not justified for the first approximation. The two reaction steps (1) and (2) are also considered to be irreversible to make the simulation as simple as possible.

This model assumes that the bulk particle is a homogeneous mixture of nitride while it decomposes. Reaction step (1) shows that production of surface nitrogen species N_{surf} is dependent only on the number of empty surface sites and a bulk concentration $N_{nitride}$, which reflects the homogeneous core approximation used in this model. Other models that consider either diffusion or heterogeneous nitride mixtures within the core will be considered subsequently.

Figure 1 displays the results of the simulation for the decomposition of γ'–Fe_4N in hydrogen. Although the rise in ammonia to the maximum rate is not well matched by the simulation, the general features of the experiment and the simulation are similar. The decay in the ammonia signal in the simulation agrees well with the experimental results, and is the result of equation (1), the conversion of nitride to surface nitrogen, dominating the rate of ammonia production. The decay curve can be made to fit exactly but at the expense of further disagreement with the rise to the maximum. The fitted parameters are given in Table 1.

The uncertainties in the parameters are measures of the sensitivity of the simulation to changes in that value. The most critical parameter is k_2, the surface reaction rate constant. A change in this parameter moves the position of the maximum, and k_2 is virtually independent of changes in the other parameters. The parameters q_1 and q_2 are included to convert the individual rate units to the normalized dimensionless concentration of NH_3 (gas phase), N_{surf} (surface), or $N_{nitride}$ (bulk). The entire success of the model is due to the choice of s_0, the fraction of empty sites, and the corresponding hydrogen surface coverage h_{surf_0} in equilibrium with this choice. At the initial exposure

Table 1

Simulation Parameters

$$N_{nitride} + s \xrightarrow{k_1} N_{surf}$$

$$N_{surf} + H_{surf} \xrightarrow{k_2} NH_3$$

parameter	units	value
k_1	$\frac{\text{mol N converted}}{\text{(mol surface atoms)(sec)}}$	23 ± 1 sec^{-1}
k_2	$\frac{\text{mol N converted}}{\text{(mol surface atoms)(sec)}}$	0.92 ± .01 sec^{-1}
q_1^*	$\frac{\text{mol surface atoms}}{\text{mol original nitride}}$	2.297×10^{-2}
q_2^*	$\frac{\text{mol surface atoms}}{\text{mol void volume}}$	6.037
s_0	$\frac{\text{mol empty sites}}{\text{mol surface atoms}}$ (time=0)	$2.0 \pm 1 \times 10^{-4}$
H_{surf0}	$\frac{\text{mol surface H}}{\text{mol surface atoms}}$ (time=0)	$\frac{0.97}{0.03} \times s_0$
N_{surf0}	$\frac{\text{mol surface N}}{\text{mol surface atoms}}$ (time=0)	$1 - H_{surf0} - s_0$

*fixed parameter for system

to hydrogen, the model predicts that the surface is virtually saturated with nitrogen, and hydrogen is limited to less than 3% of the surface. The surface reaction to form ammonia (equation 2) is limited because H_{surf} is small. As the reaction proceeds, the nitride is depleted, and the surface nitrogen decreases, causing an increase in surface hydrogen. The maximum rate of ammonia production corresponds to the point where nitrogen and hydrogen surface coverages are equal. Ammonia production thereafter decreases due to further decreases in nitrogen surface coverage. During the decay part of the curve, the conversion of nitride to surface nitrogen (equation 1) becomes kinetically important.

A number of other models were considered that did not converge on the experimental curve. The conversion of nitride to surface nitrogen, reaction (1), assumes that the concentration of bulk nitride is homogeneous within the catalyst particle and therefore diffusion does not play a role in this model. Wilson (7) has observed "bands" of nitride in intermediate samples of a ς nitride hydrogenated at 473 K, and has suggested that this represents a shrinking core of nitride, a substantially different physical picture than the homogeneous model in the simulation. Two different models were considered that incorporated the shrinking core analogy. In the first, the rate of accumulation of surface nitrogen was assumed to be a function of the area of the shrinking core (core area model), while the second model considered the concentration gradient within a particle (diffusion model). In the latter model, the surface nitrogen was given by the concentration of nitrogen at the surface as a function of radial distance from the shrinking core.

The first shrinking core model (core area) involves a reaction of nitride on the boundary of the shrinking core to nitrogen that quickly diffuses to the surface. The area of the shrinking core is simply proportional to the fraction of nitride remaining raised to the 2/3 power, and thus the original homogeneous model is simply modified by replacing $N_{nitride}$ with $N_{nitride}^{2/3}$. The results of this model are shown in Figure 2. Not only did the rise in the simulation ammonia curve not match the experimental curve, but the decay missed as well. The simulation caused the ammonia signal to fall off much faster than desired, regardless of the parameters chosen.

The second simulation (diffusion model) solved the mass transfer equation for diffusion in a solid:

$$\frac{1}{r^2}\frac{\partial}{\partial r}(D_e r^2 \frac{\partial C_N}{\partial r}) = \frac{\partial C_N}{\partial t} \tag{11}$$

where r is the radial distance in a particle, and D_e is the diffusion coefficient of nitrogen in α–Fe.

If we consider the time term as insignificant between time steps, this equation can be solved with the additional two boundary conditions

$$\text{at } r = r_e, \quad C_{Nitride} = C_{Fe_4N} \tag{12}$$

$$\text{at } r = R, \quad \text{diffusion flux} = \text{surface reaction rate} \tag{13}$$

where r_e is the radius of the shrinking core and R is the radius of the original particle. The second boundary condition simply states that the change in surface coverage is insignificant during a time step. The solution of this equation gives the concentration

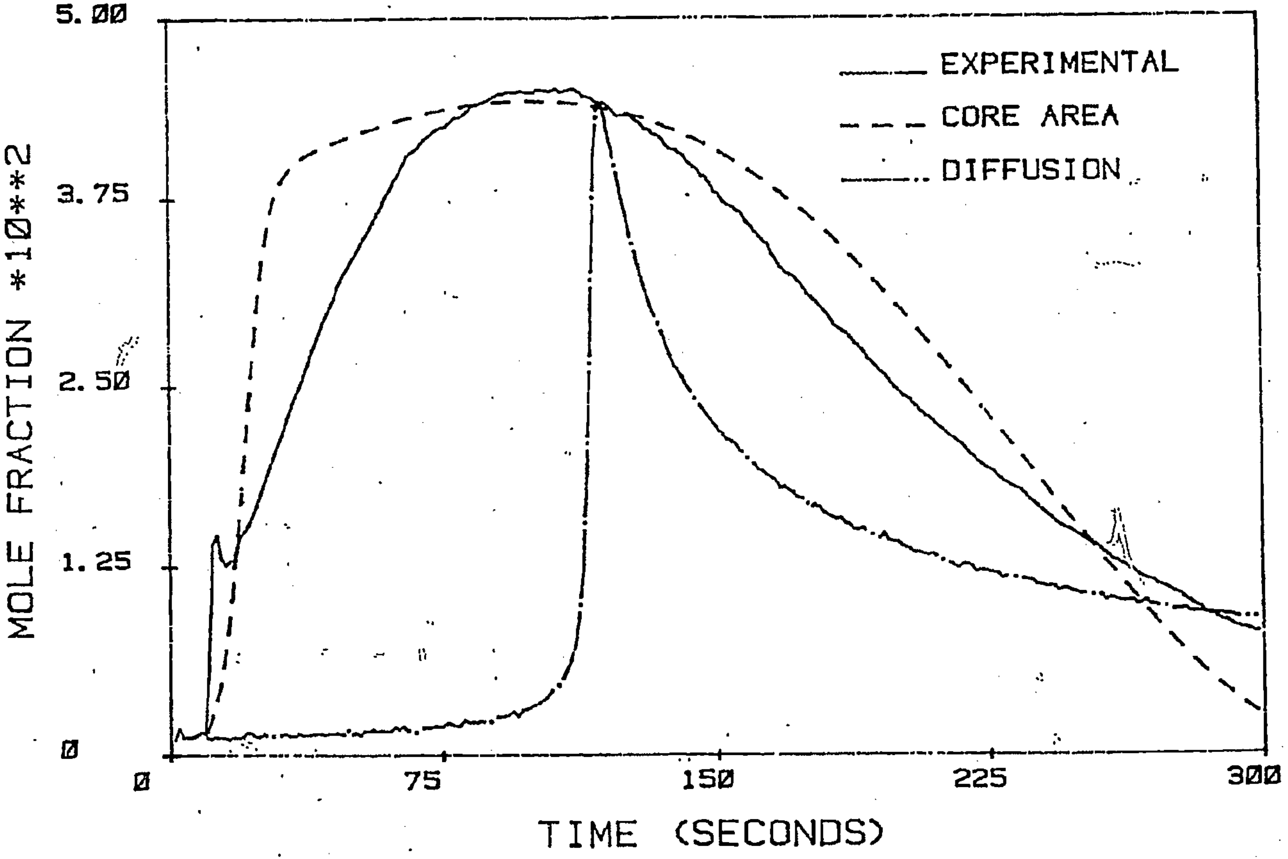

Figure 2 Simulation of the Decomposition of γ'-Fe_4N in Hydrogen: Shrinking Core Models

gradient within the particle:

$$C_{Nitride} = \frac{-A}{r} + B \qquad (14)$$

where A and B are constants in terms of the radius of the shrinking core r_e, and are given by:

$$A = \frac{R^2\, k_2\, n_{surf0}\, C_N(R)\, h_{surf}\, L}{S\, D_e\, C_N(Fe_4N)} \qquad (15)$$

$$B = C_N(Fe_4N) + \frac{A}{r_e} \qquad (16)$$

where

R = radius particle

k_2 = surface reaction rate constant

n_{surf0} = initial surface nitrogen

$C_N(R)$ = concentration of N at surface

h_{surf} = surface hydrogen

L = moles surface sites

S = surface area of total particles

The simulation calculates the radius of the shrinking core during each time step as a function of the total nitrogen removed, and then solves equation (14) to find the concentration of nitrogen at the outer surface of the particle. Schwerdtfeger has determined the diffusivity of nitrogen in various phases and reports a value of 2×10^{-10} cm^2/sec for α iron at 773 K (8). Using this value in the simulation causes complete saturation of the surface with nitrogen, regardless of the radius of the shrinking core. The radial gradient for nitrogen is near zero for this case. When the diffusivity constant is decreased to order 10^{-15} cm^2/sec, the diffusion is sufficiently slow to compete with the surface reaction. The results of this model are also shown in Figure 2. The result of this simulation is an "autoignition" point, where the increase in surface reaction accelerates the decrease in size of the core until the nitride is exhausted. The failure of this model is in its inflexibility; the other models had a reaction for nitride conversion to surface nitrogen whereas this model assumes the surface coverage is given entirely by the radial gradient in concentration. In fact, any model that relies on the boundary condition of a radial gradient determining the surface nitrogen concentration cannot predict the experimental results. As soon as the core is significantly depleted, sharp radial gradients translate into virtually no surface nitrogen, and the reaction quickly diminishes to a low rate.

A number of modifications were made to the surface reactions of the original homogeneous model in attempts to fit the experimental rise in ammonia evolution in Figure 1. These modifications included making either reaction (1) or (2) reversible and fitting rate constants for these back reactions. In neither case, however, could a satisfactory fit be achieved. Adding an extra reaction step:

$$NH_{surf} + H_{surf} \xrightarrow{k_+} NH_{2_{surf}} \tag{17}$$

provided promising results, but at the cost of missing the maximum. This simulation involved fitting 6 different parameters, including the surface coverages before introduction of hydrogen and the reaction rate constants. In all probability a sequence of reversible reaction steps, with this extra species included, would provide an exact fit of the experimental data. This simulation, however, would involve so many adjustable parameters that many sets of values could probably be found to fit the data, thereby diluting the desired goal.

The simulations have at least provided a basic mechanism by which the decomposition in hydrogen could occur. The remarkably good fit of the homogeneous nitride model with the decay curve supports the homogeneous core mechanism of equations 1 and 2. Alternatively, if the volume of the shrinking core could somehow be linearly related to the rate of nitride conversion to surface nitrogen, the simulation could accommodate this form of decomposition.

2.3 Preparation and Initial Characterization of Carbon-Supported Iron Catalysts.

a) Preparation

The nominal loading of 5 wt% iron on a carbon support was prepared by an incipient wetness technique (12). The carbon support used was Carbolac-1 (C-1), obtained from Cabot Corporation. The Carbolac was desulfurized prior to impregnation by prolonged reduction in H_2 at 1223 K for 18 hrs. The BET surface area was $1000 m^2/g$. An aqueous solution of iron nitrate ($Fe(NO_3)_3 \cdot 9H_2O$) was added dropwise and mixed between additions. The final weight loading was 4.5 wt% based on iron metal. The catalyst was air dried at RT for several days, then the nitrate ion was decomposed by reduction in H_2 (75 ml/min at 140 ° C for 4 hrs, followed by 200 ° C for 1 hr). Air was allowed to back-diffuse to the catalyst overnight to gently passivate the surface. The catalyst was sieved to 40-60 mesh to allow adequate void space between particles after compression. The self-supporting Mössbauer absorber wafer of catalyst (OD = 5/8") was composed of 160 mg of 4.5 wt% iron on carbon catalyst and approximately 100 mg of desulfurized 40-60 mesh C-1 (as a diluent). The compression was done in a hydraulic press at ~ 3000 psia.

The wafer was then mounted in the in-situ Mössbauer cell, and the cell was leak checked by pressurizing to 300 torr above atmospheric and observing any pressure change over a 30 min period. Once the cell had been found leak-free, the purge and outgas cycle was begun. First, we flushed the cell with purified He at 50 ml/min and RT for 20-30 min to remove any O_2. Next, we switched to H_2 and heated to 120 ° C to remove H_2O. The sample was reduced in flowing H_2 at 50 ml/min and 400 ° C (673 K) for 16 hrs. Following the prolonged reduction, the sample was cooled to RT, the flow of H_2 reduced, and a RT spectrum was obtained (Fig. 3a). We then exposed the sample to flowing He at RT for 21 hrs and took another RT spectrum (Fig. 3b). The sample was again reduced briefly (3hrs) in H_2 at 400 ° C prior to nitriding. The nitriding conditions were 100% NH_3 flowing at 50 ml/min at 400 ° C (673 K) for 8 hrs. The ς-Fe_2N phase was formed as is seen in the RT spectra (Fig. 3c). A premixed blend of 3:1 H_2/CO was then reacted over the catalyst wafer at approximately 1 atmosphere and 50 ml/min at 250 ° C (523 K) for 20 hrs (Fig. 3d).. Finally, the sample was rereduced in H_2 at 400 ° C for 4 hrs, cooled, and another RT spectrum obtained (Fig. 3e).

Figure 3. Mössbauer Spectra of 4.5 wt% Fe Supported on Carbolac.

a) Reduced in H_2 @400°C for 16 hrs.

b) Exposed to He @RT for 21 hrs.

c) Nitrided to ζ -Fe_2N using 100% NH_3 @400°C for 8 hrs.

d) Post - FTS @250°C for 20 hrs.

e) Rereduced in H_2 @400°C for 4 hrs.

MOSSBAUER SPECTRA 5WT% IRON ON CARBOLAC

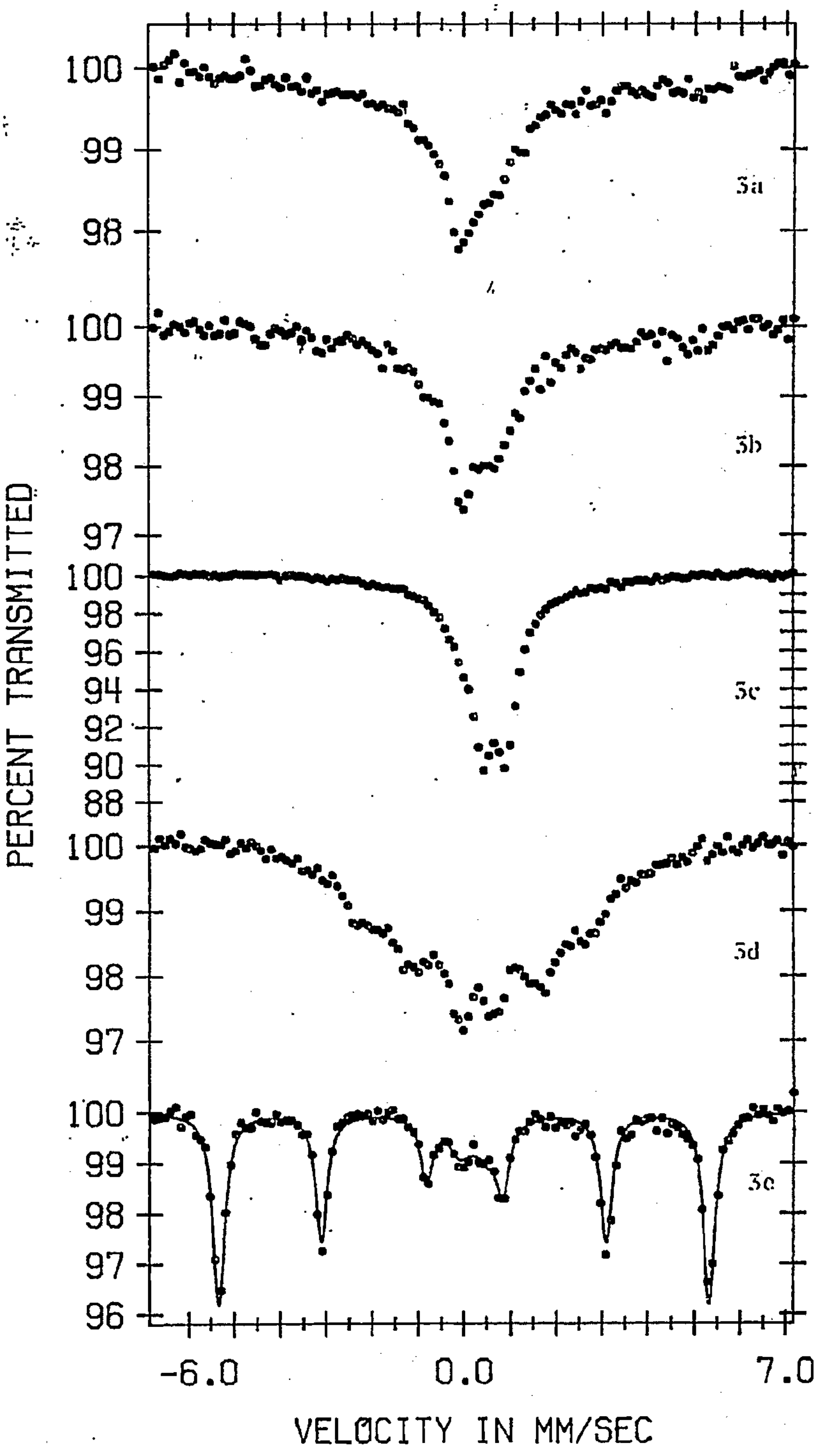

b) Mössbauer Spectra

The bowed background and broad singlet at 0.0 mm/sec shown in Fig. 3a may be ascribed to superparamagnetic Fe°. Because of thermal randomization of the nuclear spins, a magnetically split spectrum will collapse when the sample is heated above the Curie or Neel temperature or when the particle size is small such that the magnetic anisotropy energy ($KV\sin^2\theta$) is less than kT (10). In other words, the typical six line iron pattern collapses to a superparamagnetic singlet when the relaxation time is short compared to the lifetime of the excited state of the nucleus. Since our sample shows superparamagnetism at 298 K (vs 1046 K for bulk Fe), we may conclude that our iron crystallites are very small. Further work, including x-ray diffraction line-broadening and H_2 chemisorption will provide quantitative values for the size of the crystallites.

Another unusual feature of spectrum 3a is the peak at 0.8 mm/sec. We assign this peak to Fe^{2+}, which arises from incomplete reduction of the passivated iron. However, Fe^{2+} is normally a doublet with measurable quadrupole splitting, instead of a single peak. The lack of QS is the result of the fortuitous cancellation of the valence contribution to the electric field gradient with the lattice contribution (10). When the spectrum is obtained at different temperatures, the magnitude of the valence contribution to the electric field gradient changes and no longer cancels the lattice part. The singlet then splits to a doublet.

Spectrum 3b was obtained after exposure of the sample giving 3a to He at 298 K for 21 hrs. The most important feature of this spectrum is the increased absorbence of the

Fe^{2+} peak at 0.8 mm/sec. This change indicates the extreme sensitivity of highly dispersed reduced iron to trace amounts of O_2 (9). Our helium was Matheson UIIP grade (N_2,O_2,Ar,CO_2,THC as CH_4,H_2O < 10 ppm) and was further purified by two Scott Specialty Gasses Oxygen Traps, each with 99% oxygen removal efficiency. Thus, the oxygen concentration was about 1 ppb. So we see that it is risky to expose a reduced sample to helium for any length of time and therefore all subsequent spectra are taken in the gas to which the sample was exposed during pretreatment or reaction. Helium will *only* be used to passivate the samples prior to exposure to air and to purge the in-situ cell prior to treatment. The third spectrum, Fig 3c, was taken after nitriding in 100% NH_3 at 673 K for 8 hours. According to (7), this treatment should give the ζ–Fe_2N phase, which has a characteristic Mössbauer spectrum consisting of an intense doublet with IS $= 0.43$ mm/sec and QS $= 0.28$ mm/sec. Attempts to fit Fig 3c with these parameters have not succeeded. The peaks are slightly asymmetric and appear broader than previous bulk ζ–Fe_2N samples. These results may be caused by the small size and thus more heterogeneous environment of the iron phase.

The fourth spectrum, Fig 3d, was obtained following Fischer-Tropsch synthesis at 523 K for 20 hrs. This spectrum has the same general appearance of other bulk nitrided samples following FTS and indicates a complex mixture of nitride, carbide and carbonitride phases. These spectra are very difficult to fit because of the multiple overlapping patterns. Mössbauer spectroscopy at cryogenic temperatures is planned to increase the splitting of the hyperfine fields and confirm the assignments of the room temperature spectra.

The fifth and final spectrum of this series, Fig 3e, followed a re-reduction in H_2 at 673 K for 8 hrs. The obvious feature is the bulk Fe metal pattern. This fitted spectrum contains additional species with intensity near the center and accounting for 16% of the spectral area. The remaining 84% corresponds to bulk Fe with characteristic parameters. We may conclude that the iron crystallites have increased in size caused by sintering during the nitriding-reaction-re-reduction process.

c) Kinetic results

After nitriding the 5 wt% supported iron catalyst to ς–Fe_2N by exposure to 100% NH_3 at 673 K for 8 hrs and obtaining a RT spectrum in NH_3 , we heated the cell to 250 ° C (523 K) prior to beginning Fischer-Tropsch synthesis. Once the temperature had stabilized, the gas was switched to a premixed blend of H_2 and CO with a ratio of H_2 to CO of 3:1. The gasses were of UHP quality and stored in an aluminum high pressure cylinder to avoid the formation of undesirable iron carbonyls. Reaction temperature was 250 ° C (523 K) and the total pressure was approximately 1 atmosphere. The reaction products were sent to an automated gas chromatograph for analysis. Each GC analysis cycle took 40 minutes.

The olefin-paraffin ratios for C_2 's and C_3 's were high initially and then stabilized for the remaining period of time (Figures 4 and 5). The CO conversion (CO_2 -free basis) exhibited an initial peak and then a slow decline as shown in Fig 6.

Without an accurate measure of iron crystallite size, we cannot accurately calculate turnover frequencies for comparison with literature values. However, since we know

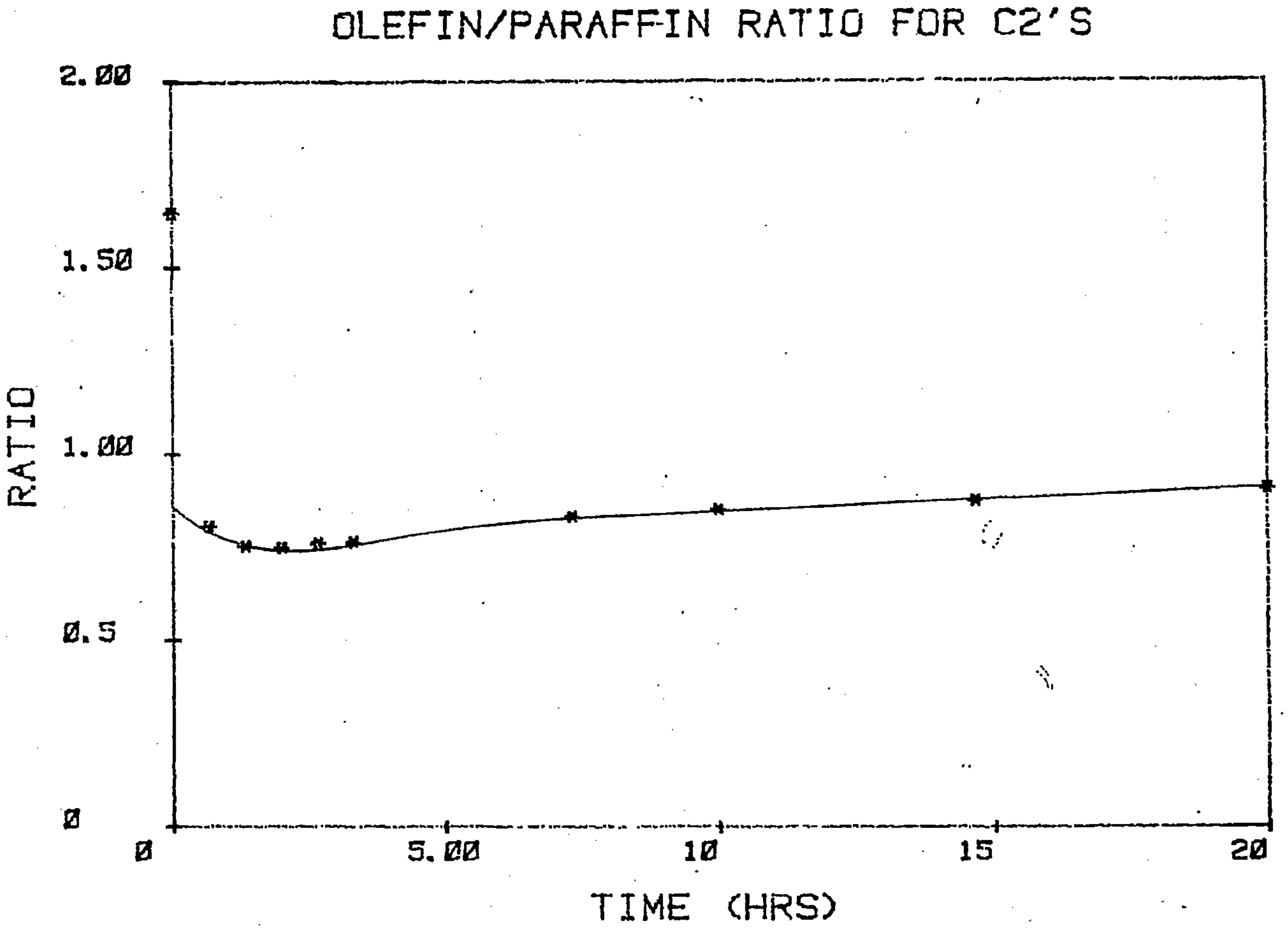

Figure 4. Olefin to Paraffin Ratio for C_2's from Supported ζ -Fe_2N Catalyst

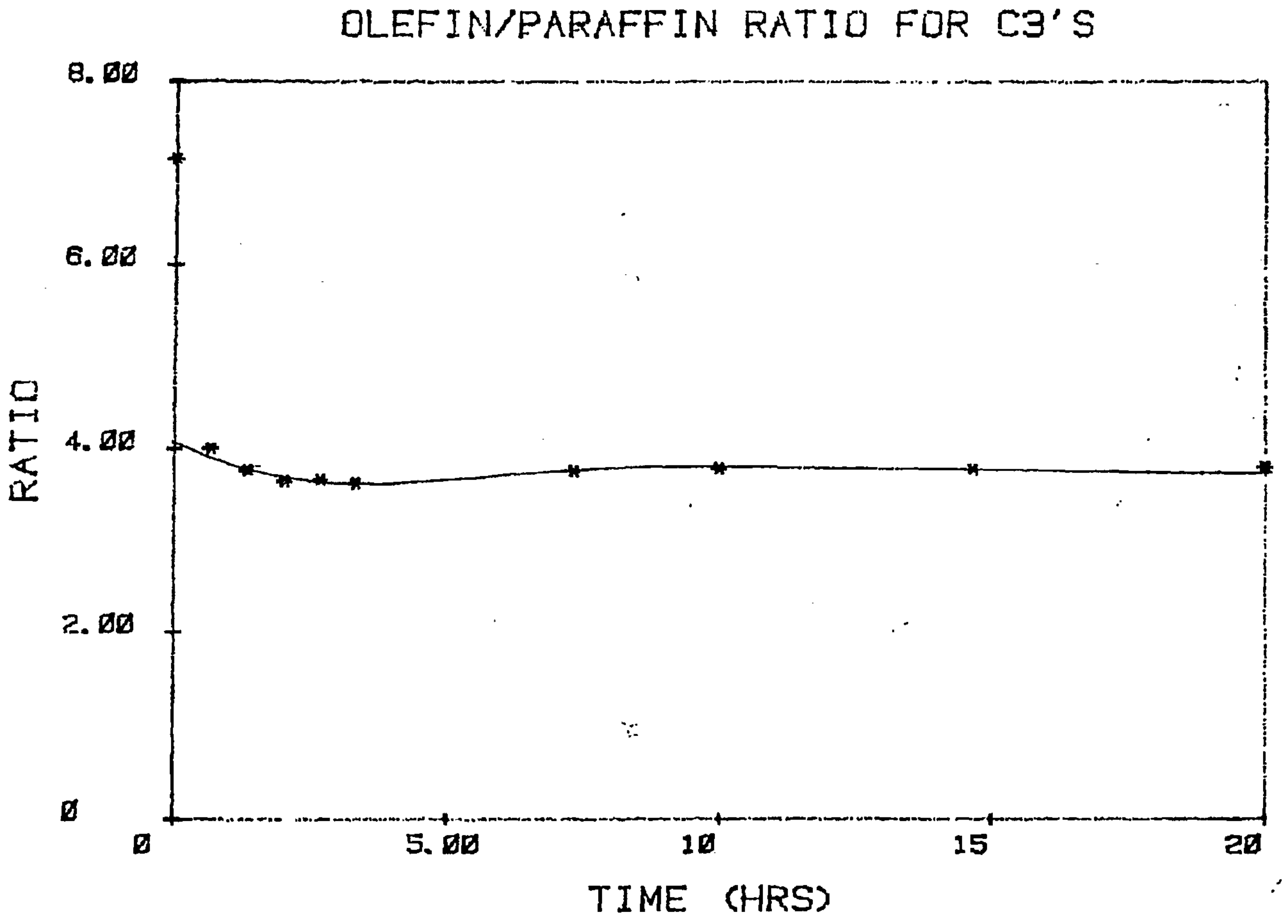

Figure 5. Olefin to Paraffin Ratio for C_3's from Supported ζ -Fe_2N Catalyst.

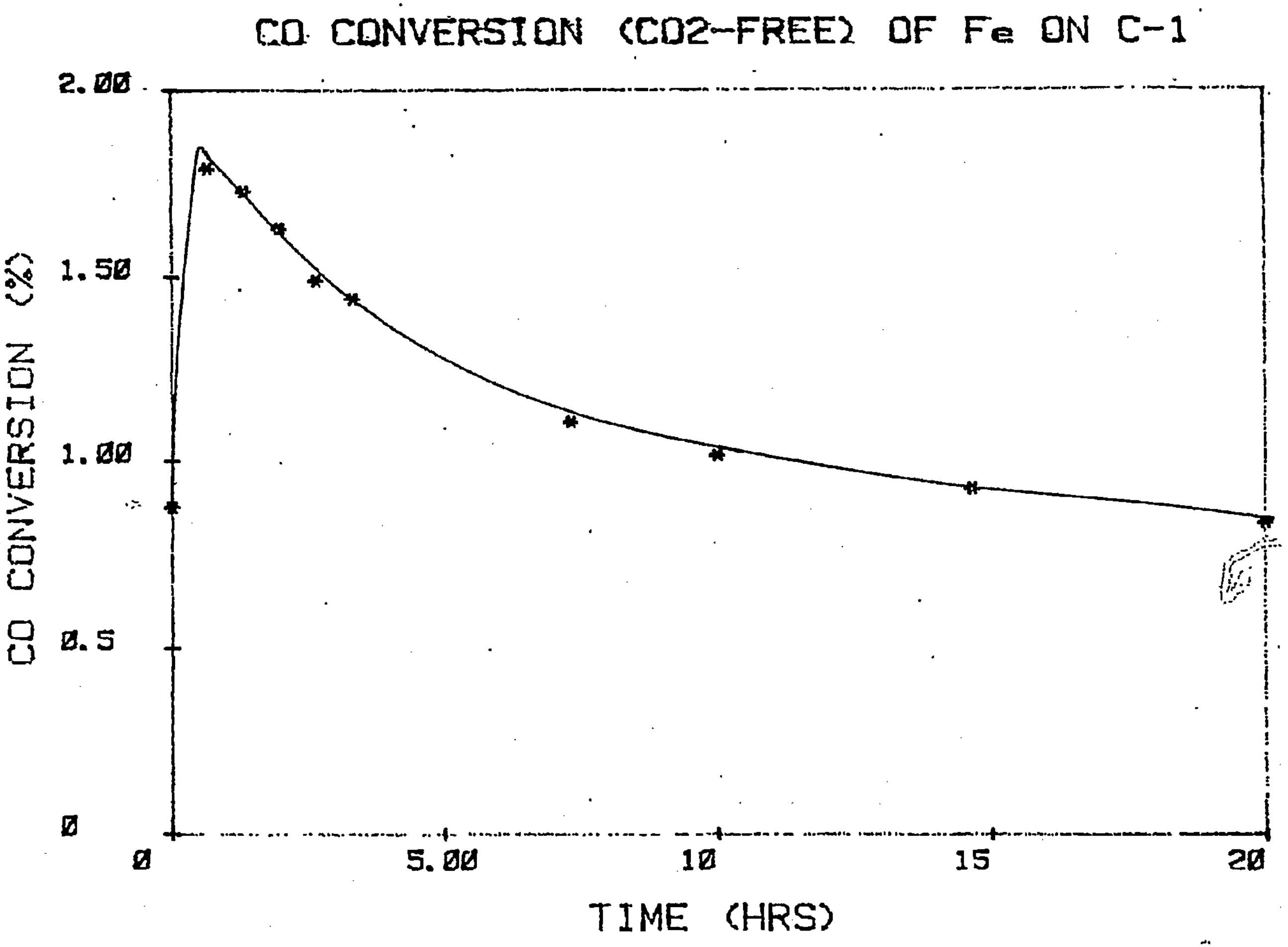

Figure 6. CO Conversion (CO_2 -free basis) from Supported ζ -Fe_2N Catalyst.

that the iron particles are small, we estimate their size to be 25 Å . Using this value we calculate the turnover numbers at the maximum to be $7\text{x}10^{-3}\ \frac{\text{molecules}}{\text{sitesec}}$. This number is slightly below the value of $4\text{x}10^{-2}$ found for the bulk nitride and is consistent with the findings of Vannice et al that the specific rates for small iron particles on carbon are slightly below values formed for more conventional iron catalysts (9). We also note that the decline in activity after a maximum is different from the steady rates found for unnitrided Fe/Carbolac. The decline may well be related to the sintering observed after rereduction and will be examined in further detail.

FUTURE RESEARCH

We will computer fit the Mössbauer spectra in Figure 3 using our new fitting program which uses combinations of elementary subspectra. This program avoids the multiple linear constraints which must be imposed on the old program to yield physically meaningful parameters, and also allows for distributions of parameters. The next task will be to prepare supported iron catalysts having higher weight loadings and correspondingly larger particle sizes. The average particle size will be determined by x-ray diffraction line broadening, Mössbauer spectroscopy, and selective H_2 chemisorption. After nitriding these catalysts, we will study the effect of particle size on catalyst activity and selectivity. We also plan to confirm the altered selectivity following preoxidation of a nitrided catalyst, which was discussed in an earlier report. We will begin by repeating the procedure on a bulk iron catalyst and later extend these experiments to supported iron catalysts.

REFERENCES

1. Anderson, R.B., Cat.Rev. Sci. Eng. *21,* 53 (1980).
2. Olive', G. and Olive', S., U.S. Patent 4, 179, 462, Dec. 18, 1979.
3. Gambell, J.W. and Auvil, S.R., U.S. Patent 4, 272, 451, June 9, 1981.
4. Auvil, S.R. and Penquite, C.R., U.S. Patent 4, 272, 452, June 9, 1981.
5. U.S. Department of Energy Quarterly Technical Progress Report, DOE/PC/50804-5.
6. Benziger, J. and Madix, R.J., Surf. Sci., *94,* 119 (1980).
7. Wilson, A., M.S. Thesis, Purdue University (1984).
8. Schwerdtfeger, C., Grieveson, P. and Turkdogon, E.T., Trans. Met. Soc., *245,* 2461 (1969).
9. Jung, H.J., Vannice, M.A., Mulay, L.N., Stanfield, R.M. and Delgass, W.N., J, Cat., *76,* 208 (1982).
10. Niemantsverdriet, J.W., van der Kraan, A.M., Delgass, W.N. and Vannice, M.A., J. Phys. Chem., *89,* 67 (1985).
11. Yeh, E.B., Schwartz, L.H. and Butt, J.B., J. Cat., *75,* 241 (1985).
12. Jung, H.J., Walker, P.L. and Vannice, M.A., J. Cat., *75,* 416 (1982).

APPENDICES

Distribution List

A) *Fred W. Steffgen* (3)
Project Manager
U.S. Department of Energy Pittsburgh Energy Technology Center
P.O. Box 10940
Pittsburgh, PA 16236

B) *Michael Hogan*
Acquisition & Assistance Division
U.S. Department of Energy
Pittsburgh Energy Technology Center
P.O. Box 10940
Pittsburgh, PA 16236

*C) U.S. Department of Energy
Technical Information Center
P.O. Box 62
Oak Ridge, TN 37830

E) U.S. Department of Energy
Patent Office
Office of General Counsel
Chicago Operations & Regional Office
9800 South Cass Avenue
Argonne, IL 60439

G) *Frank M. Ferrell, Jr.*
U.S. Department of Energy Fe-3 MS C-156 GTN
Washington, D.C. 20545

H) *Marilyn Keane* (3)
U.S. Department of Energy
Pittsburgh Energy Technology Center
P.O. Box 10940
Mail Stop 920-116
Pittsburgh, PA 15236

I) *A.A. Hummel*
Graduate Student
School of Chemical Engineering
Purdue University

J) *K. Hummel*
Graduate Student
School of Chemical Engineering
Purdue University

K) *Jerry L. Arnold*
Principal Research Metallurgist
Research and Technology
ARMCO Inc.
703 Curtis Street
Middletown, OH 45043

*Note: Grantee Shall obtain patent
clearance from
addressee "E" above
prior to forwarding
copies to TIC.
Include Statement
"Patent Cleared by
Chicago OPC on

______________"
Date

Reproduced by NTIS

National Technical Information Service
Springfield, VA 22161

This report was printed specifically for your order from nearly 3 million titles available in our collection.

For economy and efficiency, NTIS does not maintain stock of its vast collection of technical reports. Rather, most documents are custom reproduced for each order. Documents that are not in electronic format are reproduced from master archival copies and are the best possible reproductions available.

Occasionally, older master materials may reproduce portions of documents that are not fully legible. If you have questions concerning this document or any order you have placed with NTIS, please call our Customer Service Department at (703) 605-6050.

About NTIS

NTIS collects scientific, technical, engineering, and related business information – then organizes, maintains, and disseminates that information in a variety of formats – including electronic download, online access, CD-ROM, magnetic tape, diskette, multimedia, microfiche and paper.

The NTIS collection of nearly 3 million titles includes reports describing research conducted or sponsored by federal agencies and their contractors; statistical and business information; U.S. military publications; multimedia training products; computer software and electronic databases developed by federal agencies; and technical reports prepared by research organizations worldwide.

For more information about NTIS, visit our Web site at **http://www.ntis.gov**.

NTIS

Ensuring Permanent, Easy Access to U.S. Government Information Assets

SATISFACTION GUARANTEED

NTIS strives to provide quality products, reliable service, and fast delivery. Please contact us for a replacement within 30 days if the item you receive is defective or if we have made an error in filling your order.

- **E-mail: info@ntis.gov**
- **Phone: 1-888-584-8332 or (703)605-6050**

U.S. DEPARTMENT OF COMMERCE
Technology Administration
National Technical Information Service
Springfield, VA 22161 (703) 605-6000